California Institute of Technology

Seismological Laboratory

Pasadena, California 91125

Develop Design Criteria for Penetrator Emplacement of a Multi-Station Seismic Experiment

FINAL REPORT

April 18, 1977

National Aeronautics and Space Administration

Contract NSG-7160

Final Report, Contract NSG 7160

April 18, 1976

Develop Design Criteria for Penetrator Emplacement of a Multi-Station Seismic Experiment

Introduction

During the period covered by this contract (July 1, 1975 to June 30, 1976) a number of studies and experiments have been undertaken which are preliminary to the development of a penetrator-emplaced seismic station. Specifically we have: 1. Studied triaxial transducer designs which will fit within the required envelope; 2. Conducted pier tests on two commercially available accelerometers; 3. Shock tested one of the commercially available accelerometers, an inertial mass-suspension system of our own design and some candidate centering motors at the Sandia Laboratory shock test facility.

Candidate Instrument Designs

Figures 1 through 4 are schematic representations of instruments which we feel are good candidates for meeting the requirements of volume and sensitivity. All are designs which are based on instruments which we have built in the past for other applications. Most of the designs are shown without transducers or facilities for damping. It is anticipated that displacement transducers will be used in each design because of their greater response at very low frequencies over that of velocity transducers. However, velocity transducers are not ruled out and, in fact, an auxiliary velocity transducer (coil and magnet) may be added as part of a feedback design used for instrument centering and stabilization.

Viscous damping will be achieved by liquid filling the instrument, this also acts as a protection against the forces of acceleration experienced upon impact with the planetary surface. In addition, the liquid may serve as the dielectric for a capacitive bridge transducer or as the conductive media for a resistive bridge transducer. Liquid viscous damping, provided the components are properly designed, is proportional to velocity, as is electro-magnetic damping; however, the elimination of magnetic devices will avoid stray magnetic fields which might adversely affect other experiments aboard the penetrater.

Figure 1 shows a coaxial, triaxial suspension based upon a design previously used as a compact down-hole system. Resistive or capacitive bridge transducers are shown. A negative length spring will be used on the vertical to effect the equivalent of a greater spring extension in the small envelope and the period may be lengthened by incorporating an iron disk on the mass with a small magnet fixed to the frame. This technique is shown in more detail in Figure 2.

The vertical component shown in Figure 2 is, in principle, identical to the vertical component in Figure 1. The biaxial horizontal instrument is a simple pendulum with period lengthening. A model of this design has been constructed to demonstrate the technique. The attraction between the magnet on the mass and the iron ring on the frame effects the cancellation of system restoring force with the resultant increase in the natural period from 0.3 sec to 1.0 sec. Because the instrument period varies inversely as the square of the restoring force, 0.9 of the system restoring force is transferred to the frame. Thus, an auxiliary displacement transducer may be

added by the addition of force sensing transducers between the iron ring and the frame. The horizontal components shown in Figure 3 incorporate a biaxial, inverted pendulum.

Whatever suspension system is finally selected, the design must be capable of withstanding the forces encountered upon impact. This may be accomplished by using a rigid caging system as was done in the Viking instrument, or by building compliance into the suspension. An example of this latter technique, applied to an inverted pendulum, is shown schematically in Figure 4. Here the acceleration force is transferred to a limit stop. This design was constructed and shock tested to a peak acceleration of 2200 g (acceleration waveform shown in Fig. 5A) at the Sandia Laboratory shock test facility with no detrimental effects.

As was mentioned, all of the designs discussed would use fluid damping and this fluid may also act as an electrolyte between transducer plates and the common mass. The variable resistance of the electrolyte would form two arms of an alternating current bridge. This is the form of the transducer used with the biaxial bubble tiltmeter, still to be discussed and such a transducer was tested on the inverted pendulum design. An electrical schematic of the bridge circuit is shown in Figure 6 for two axis. Although the commercial bubble tiltmeter uses a common carrier oscillator, different frequencies on each axis would help eliminate cross-coupling of the axes.

Bubble Tiltmeter

Our studies of transducers applicable to a penetrator has also included commercially available units, two of which seem promising. The first of these is the Autonetics Model SE541A biaxial tiltmeter, shown in Figure 7.

In principle, the tiltmeter sensor is simply the ancient spirit level, in which the position of the bubble or void in a body of fluid is used to indicate the attitude of the fluid container with respect to gravity. The fluid is a methyl or ethyl alcohol or an alcohol and glycerin mixture. The position of the bubble is detected by a resistive bridge, as previously discussed. The weight of the bubble assembly is approximately 25 grams and its power consumption less than 0.1 milliwatt.

According to the manufacturer, the limit of resolution is of the order of 4×10^{-7} degree at 1 Hz which is equivalent to 7×10^{-9} g. The small size biaxial nature and high sensitivity make it a good candidate for a seismic instrument aboard a penetrator. A unit was subjected to the standard checkout calibration by the manufacturer and then packaged in a jig and shock tested at Sandia to a peak value of 700 g (Figure 5b). It was then submitted to the manufacturer for recalibration and found to be within the initial calibration specifications.

Force Balance Accelerometer

The other commercial accelerometer which we have investigated is the Systron-Donner force balance accelerometer, Model 4841. The primary application of this device is as a strapdown sensor for guidance systems. A drawing of the unit is shown in Figure 8 along with an operational block diagram. The inertial pendulum is maintained nearly at its mechanical zero position by the high gain amplifier and servo loop. This unit is primarily a high frequency (greater than 50 Hz) device, so much of our effort was to determine its low frequency characteristics.

If this unit has sufficient sensitivity for the application it is of

particular interest to us because of its inherent feedback. We anticipate including signal shaping circuitry in the feedback loop and thus may control the low frequency response of the device in the manner discussed in our previous reports on this subject. The weight of the unit is roughly 250 grams per axis and the power consumption of the electronics supplied by the manufacturer is about 120 mw. The suspension of the inertial mass is by a diamond bearing which the manufacturer claims is purely elastic; however, with our pier testing we were unable to verify this.

Pier Tests

Both the Autonetics bubble tiltmeter and the Systron-Donner accelerometer were pier tested with their seismic recordings compared to standard instruments. We have two test sites, one on the CIT campus and one at the CIT Kresge Laboratory about 4 km west of the campus. The bubble was simultaneously tested at the Kresge and campus sites. At the Kresge facility the bubble's frequency response was shaped electronically to equal the magnification of a Benioff 1-90 system over the range of roughly 2 sec to 20 sec (Figure 9) to determine its long period characteristics. At the campus facility, very little response shaping was used so that its short period and wideband characteristics might be compared to the Viking instrument, a more or less conventional geophone (Figure 11). The force balance accelerometer was also tested at the campus site and compared against the Viking and bubble instruments.

Figure 10 shows a Peruvian earthquake of magnitude 6 3/4 recorded at Kresge on the bubble and the Benioff system. Figure 10a and 10b show the beginning of the event (time scales are not the same on the two recordings)

and Figures 10c and 10d show long period waves arriving some 13 minutes later. Figure 12 compares the short period characteristics of the bubble with the Viking for a local event. The wide band characteristics of the bubble are evident as indicated by the presence of 6 sec microseisms, which are absent on the Viking record, and the high frequency signatures of the local event and the train. Also shown, in Figure 12a, is a record of the same event as it appears after being processed by the Viking data compression system. This system extracts the envelope of the event and also makes a count of the number of times the signal made a position crossing of the zero axis, as a measure of the harmonic content of the event. The sampling interval in each case is one sample per second. Some kind of data compression will also be needed for the seismic penetrator experiment.

A comparison of the Viking instrument, the bubble and the force balance accelerometer is made in Figure 13 for a teleseism. Here again, the wide-band characteristics of the bubble are evident. The record of the force balance accelerometer, however, is disturbing due to the lack of 6 sec microseisms. The response curves of Figure 11 show that in the region of 6 seconds (arrows) the response of the bubble and the force balance accelerometer should be within a few db. However, Figure 13 and other recordings of the force balance accelerometer, do not show 6 sec microseisms, indicating that the response is not as shown in Figure 11. The 6 sec microseisms represent an acceleration of the order of 10^{-7}g and their absence on the record could be interpreted to mean that the diamond suspension of the force balance accelerometer is not purely elastic at these g levels, perhaps resulting in the existence of a break-away threshold. Records supplied by Systron-Donner, however, seem to show 6 sec microseisms although no comparison

instrument was operated at the time the recordings were made. This question remains unresolved; however, problems in the instrumentation are not ruled out.

Leveling Motors

This laboratory has had experience with high acceleration testing of conventional seismometer components including d.c. permanent magnet motors and gear trains, dating back to the development of the Ranger Lunar seismometer in the 1960's (Lehner, et al., 1962). Under this program, components were tested up to 10,000 g. One type of component, not available at the time, which might be applicable to the leveling and centering of a seismometer is the stepping motor. These may be obtained in a small size and can provide a fine incremental shaft rotation with little or no gear train.

The speed-torque and speed-power characteristics of a trio of Computer-Devices permanent magnet stepping motors, Model No. 08M-01X, were measured and the motors mounted in a jig, shown in Figure 14, so that two of the motors would be shocked coaxially with the motor shafts, one from the front and one from the rear, and the third motor shocked transverse to the shaft. The units were subjected to a shock of 2100 g (Figure 5c) and retested with no significant changes in their tested characteristics.

Summary

Figure 15 is from one of our previous reports and shows what we thought could be accomplished with an advanced Viking type instrument or what would have to be done in order to extend its response to that necessary to observe the free modes of Mars. The dotted area at 10^{-7} g has been added to indicate

the response of the bubble that we have demonstrated. It may, in fact, have much greater sensitivity than this since the manufacturer claims a resolution of greater than 10^{-8} g at a 1 Hz bandwidth. If the lack of 6 sec microseisms on the recordings from the force balance accelerometer is in fact due to instrumentation problems, it too, would have a response within the dotted area in Figure 14 and a shock test of this instrument would be in order.

Reference

Lehner, et al., A Seismometer for Ranger Lunar Landing, Final Report to NASA Contract NASw-81, May 15, 1962.

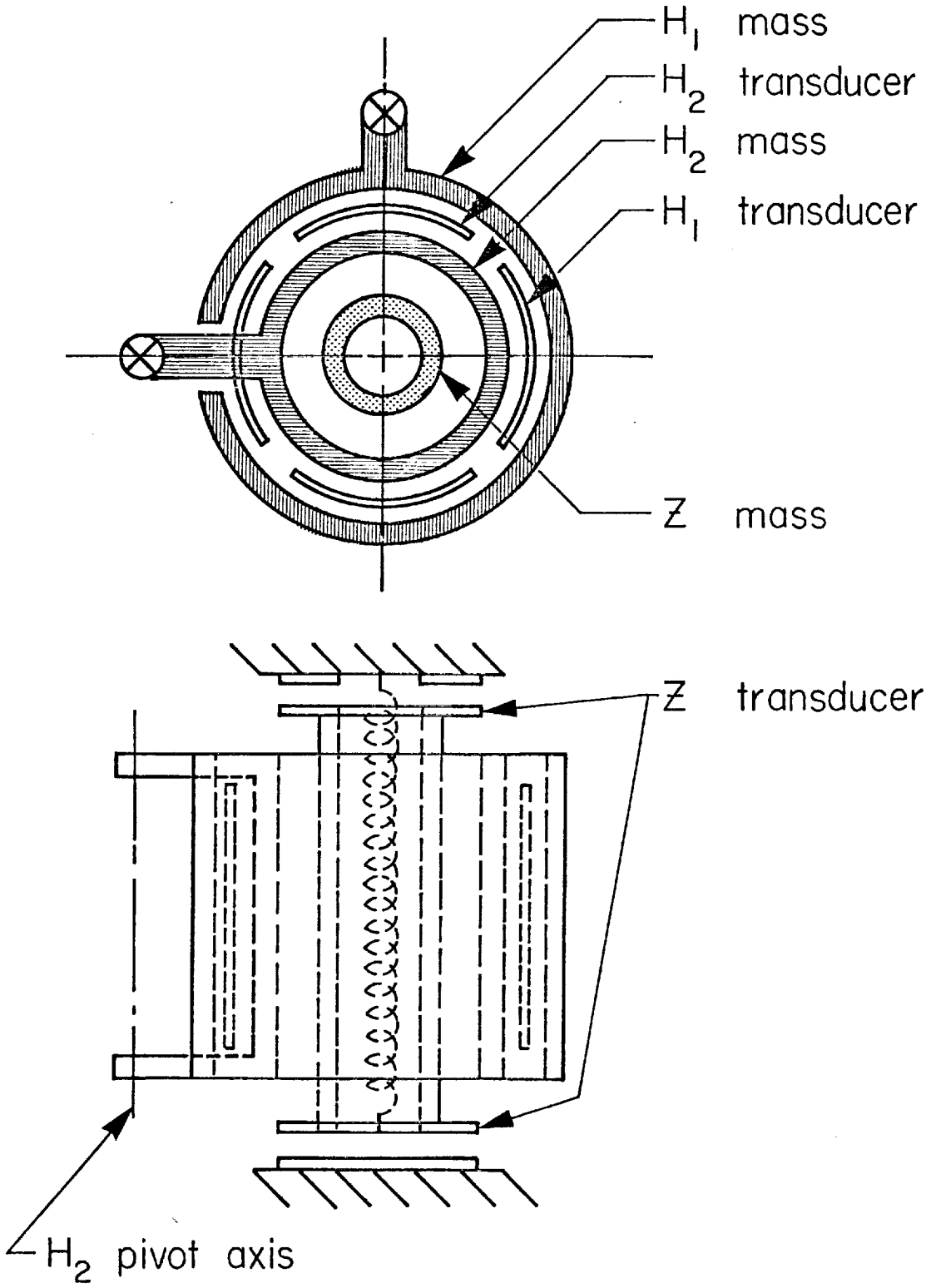

Triaxial Suspension System

FIGURE 1

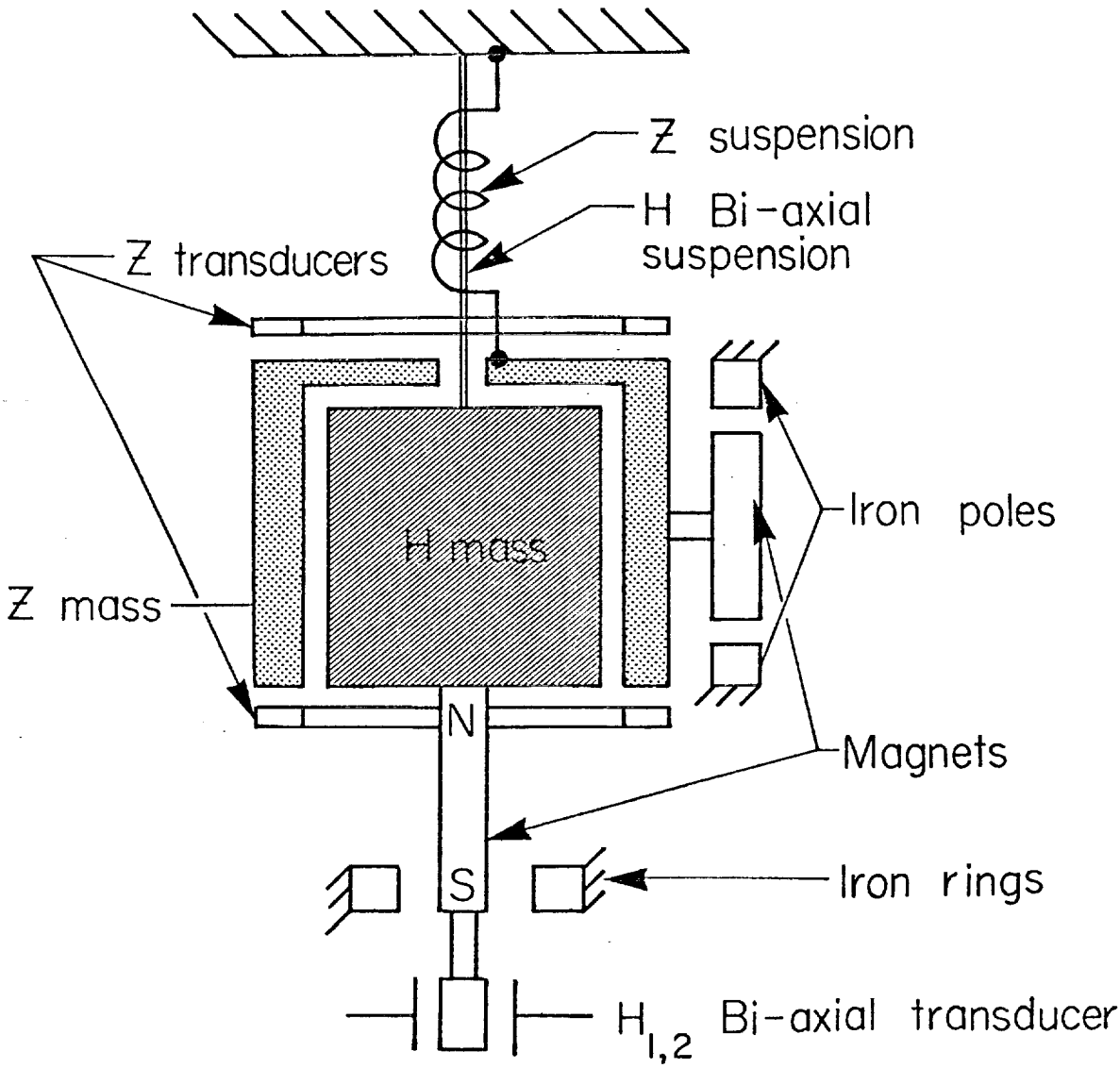

Triaxial Suspension System
with period lengthning

FIGURE 2

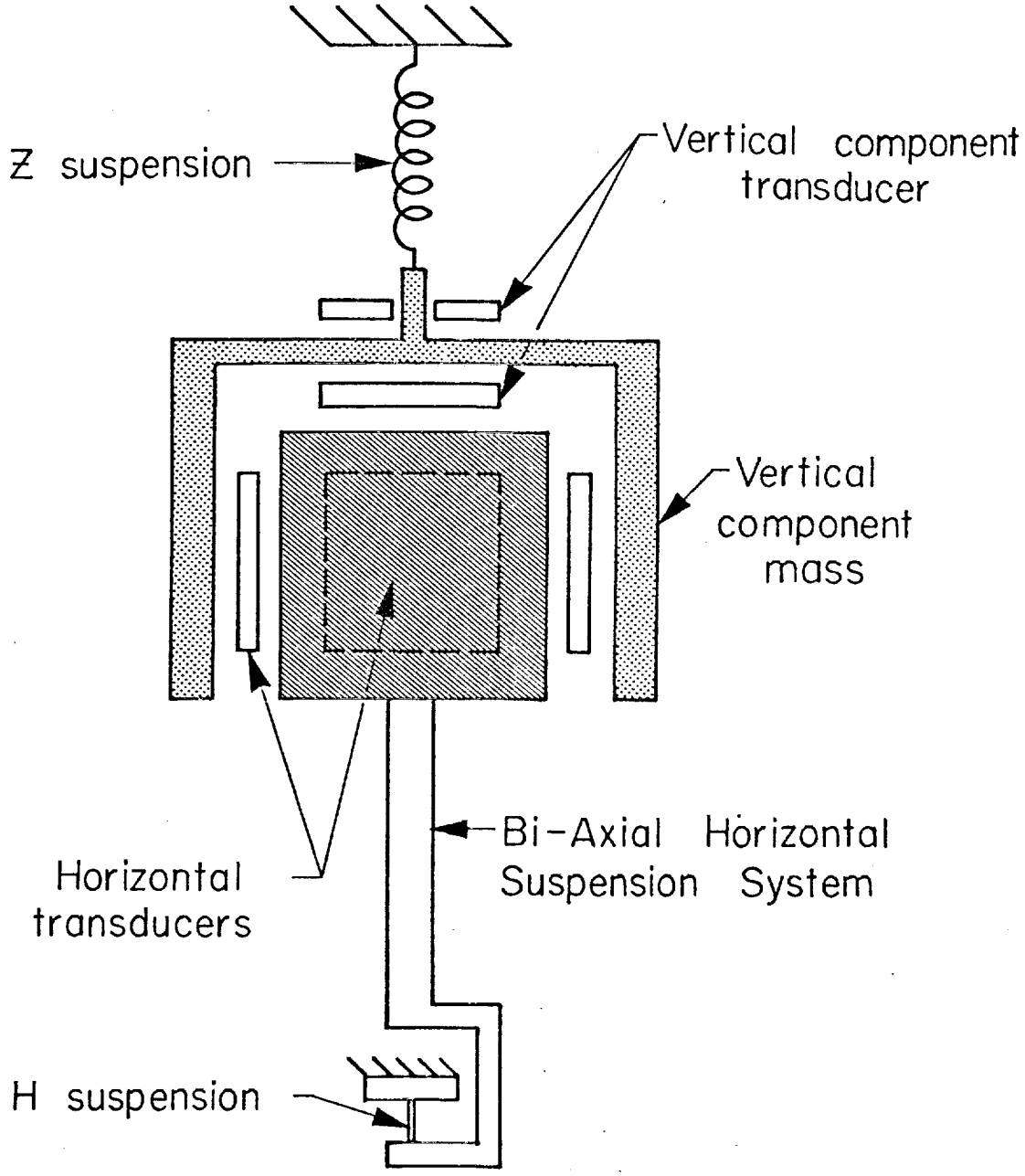

Triaxial Suspension System

FIGURE 3

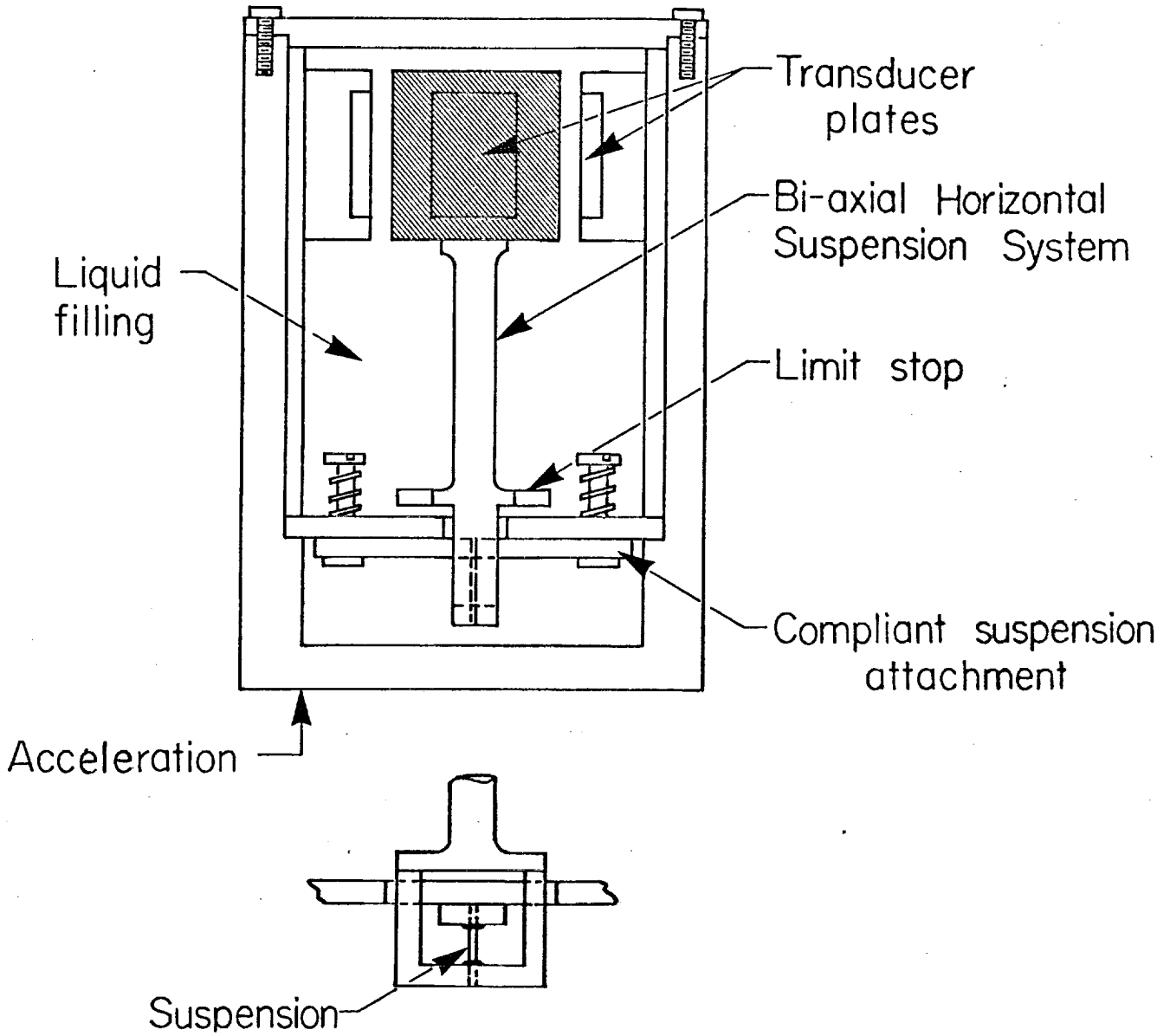

Experimental Bi-axial Horizontal Seismometer

FIGURE 4

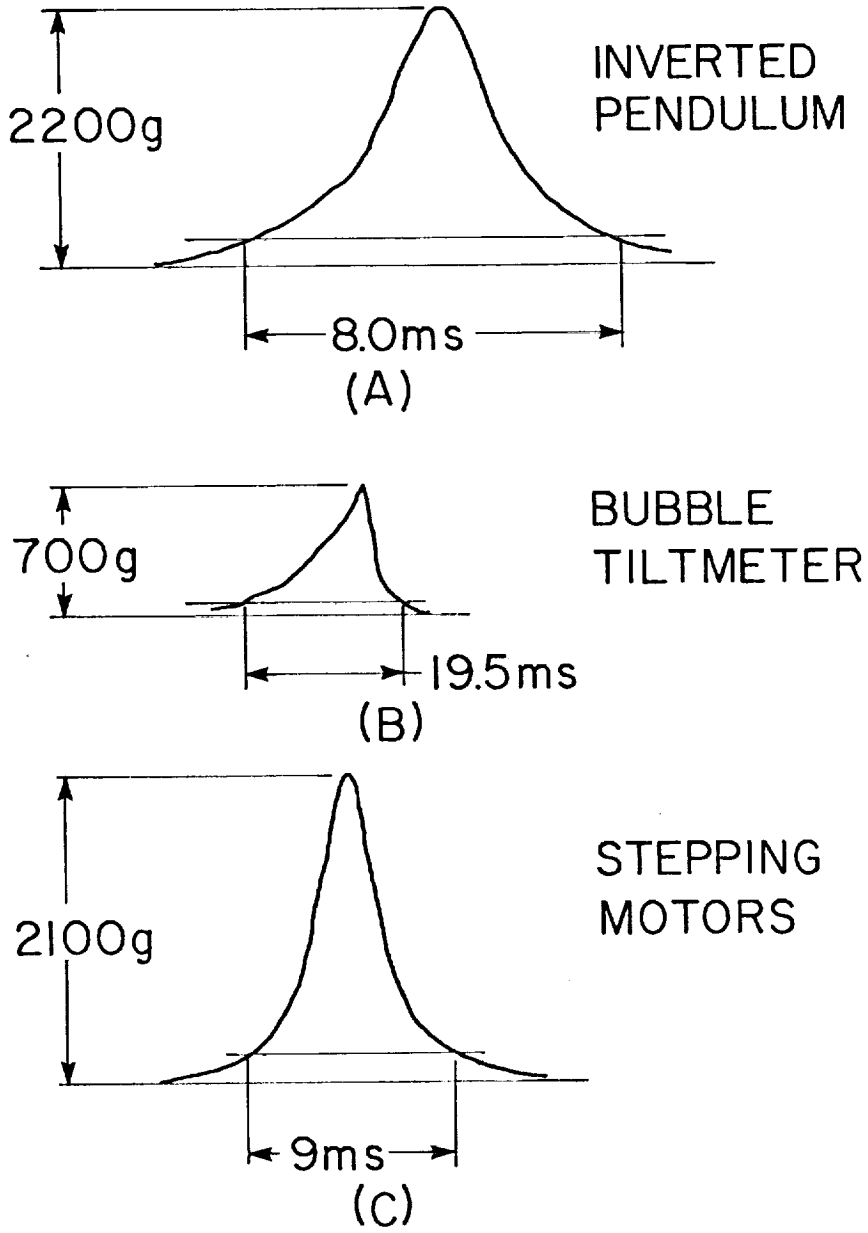

ACCELERATION WAVEFORMS OF SHOCK TESTS CONDUCTED AT THE SANDIA LABORATORY SHOCK TEST FACILITY. TIME IS DEFINED AS THE TIME THE ACCELERATION IS ABOVE 10% OF THE PEAK VALUE. (FIGURES NOT TO SAME SCALE)

FIGURE 5

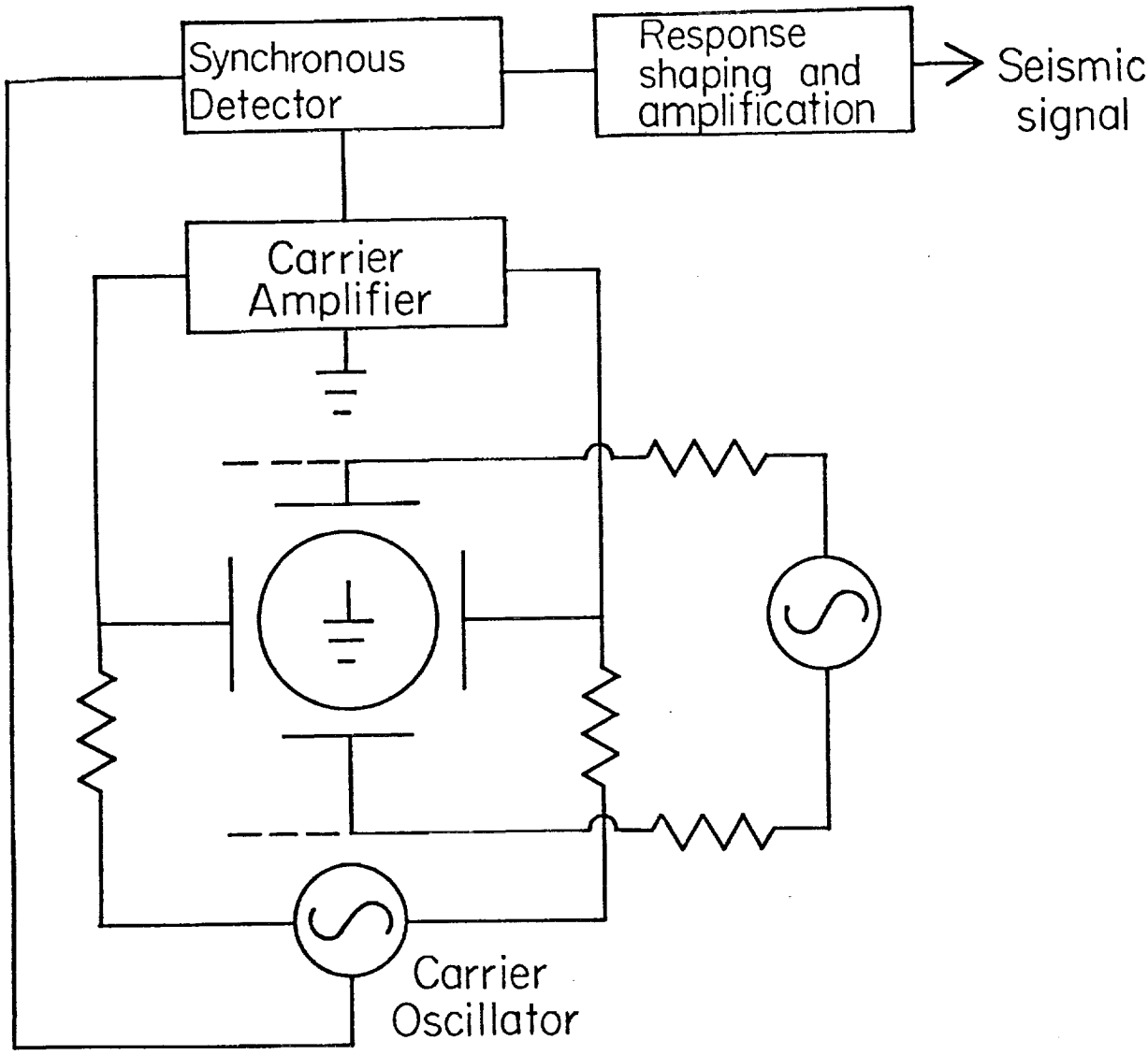

Seismometer System Block Diagram

FIGURE 6

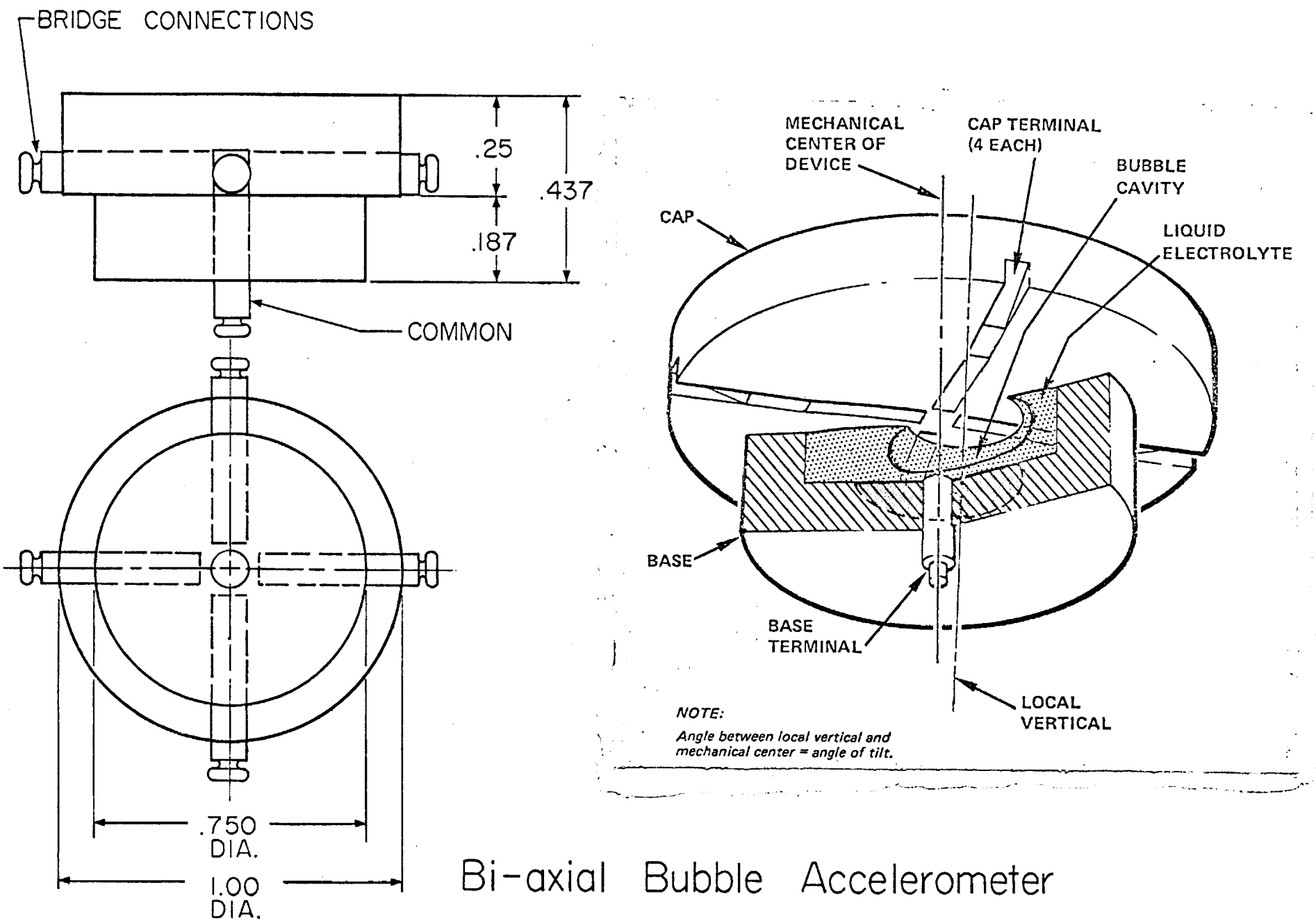

Bi-axial Bubble Accelerometer

FIGURE 7

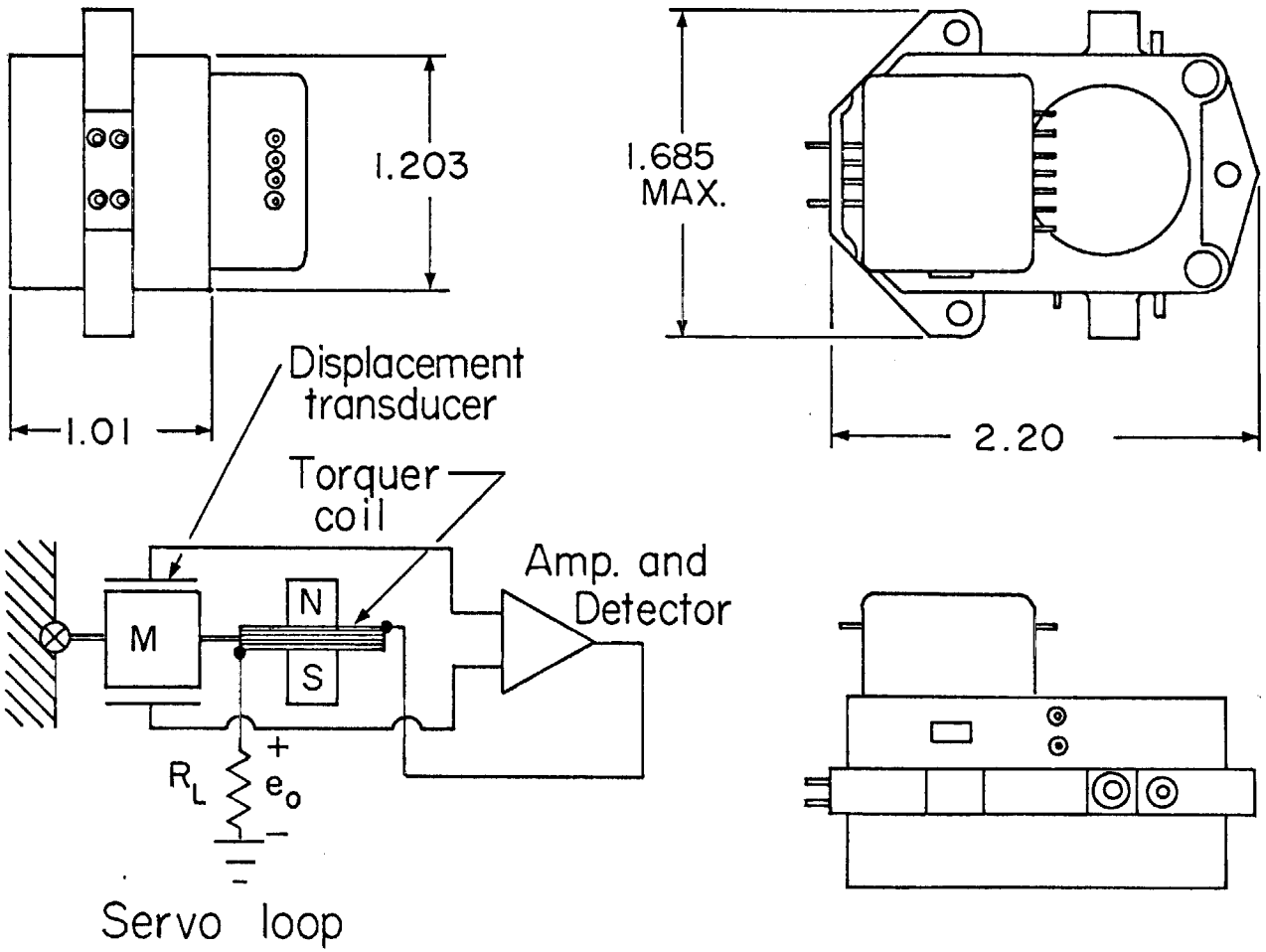

Force Balance Accelerometer

FIGURE 8

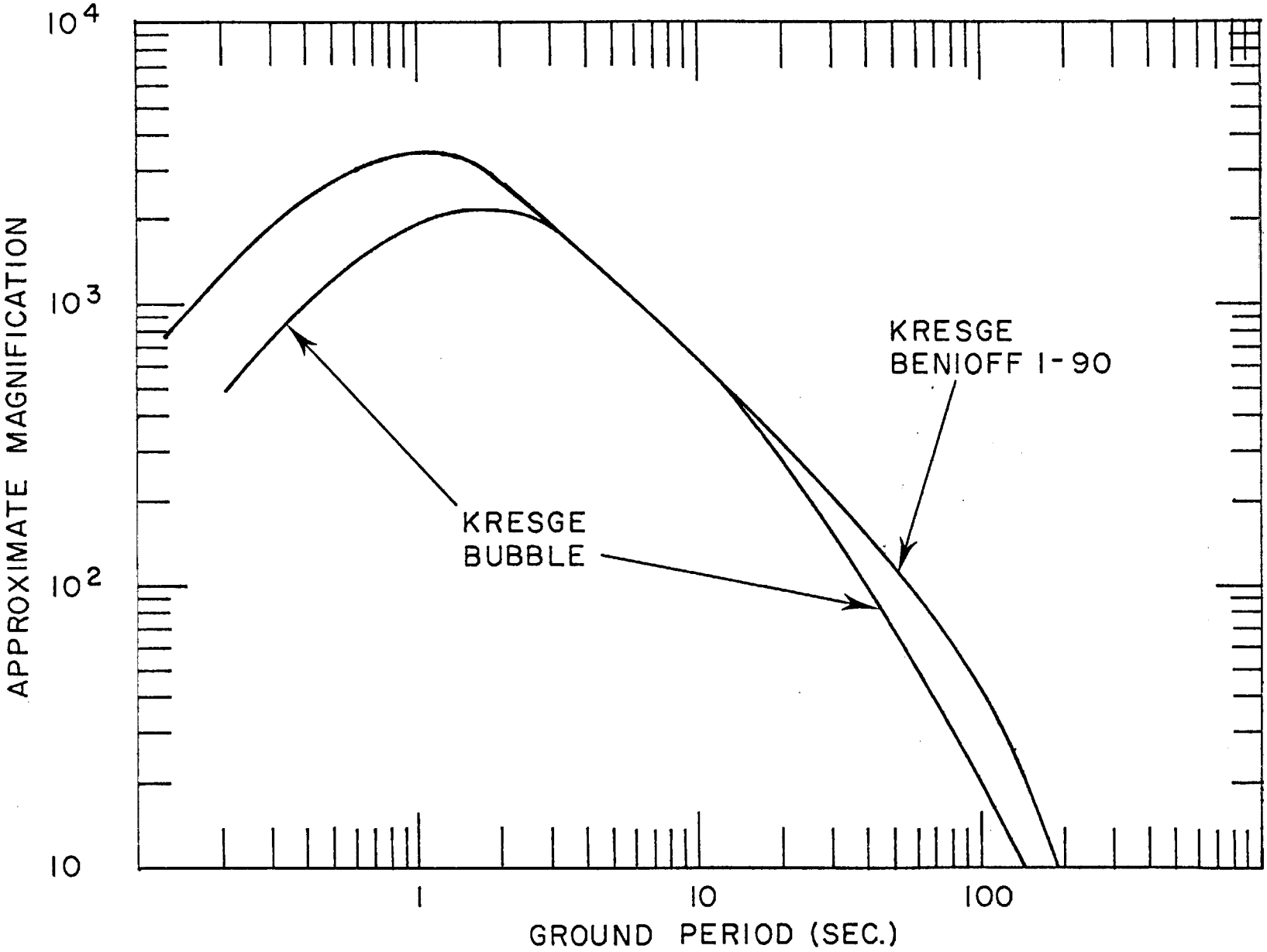

COMPARISON CHARACTERISTICS AT KRESGE TEST SITE

FIGURE 9

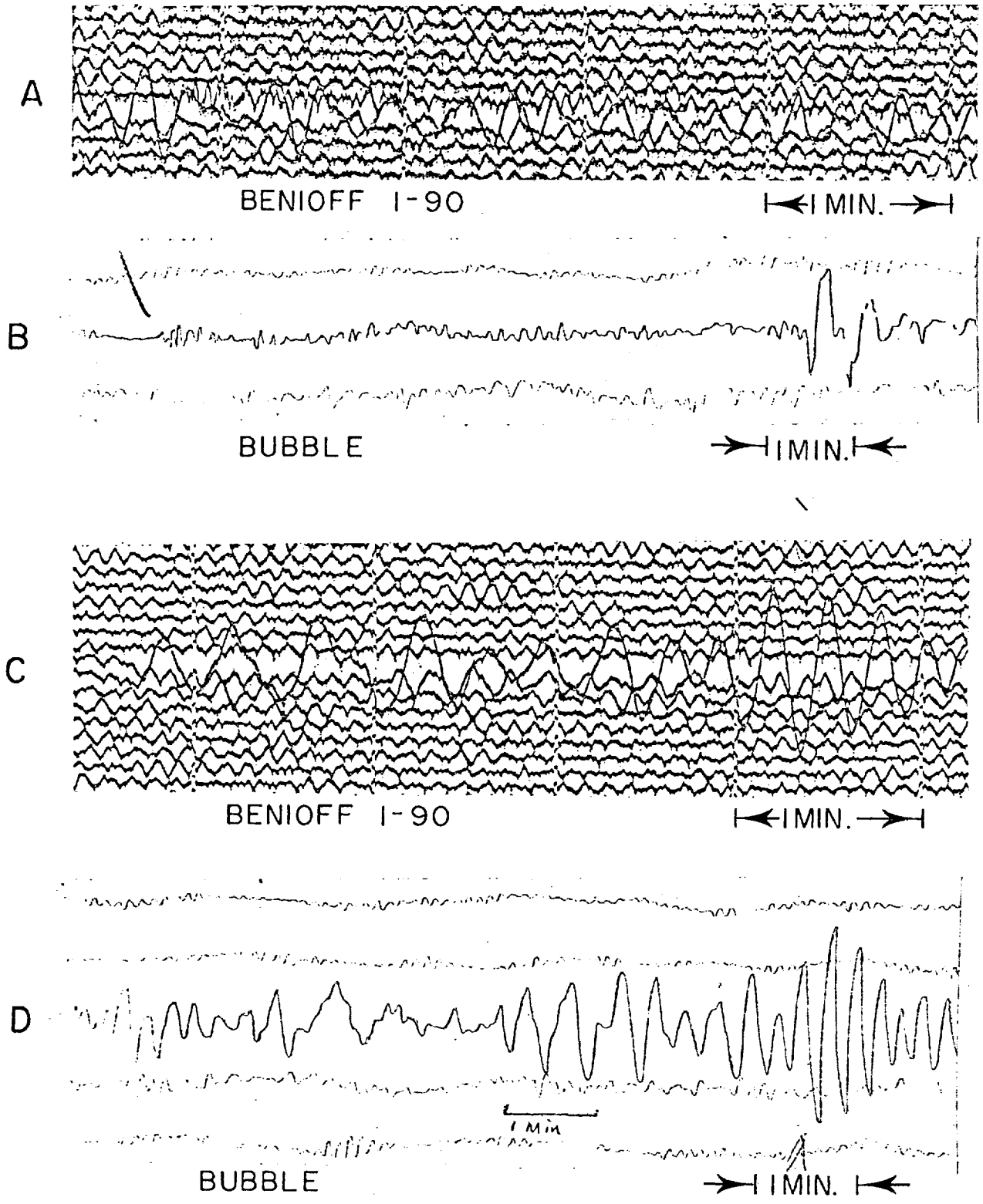

MAGNITUDE 6 3/4 (PERU) RECORDED AT KRESGE TEST SITE

FIGURE 10

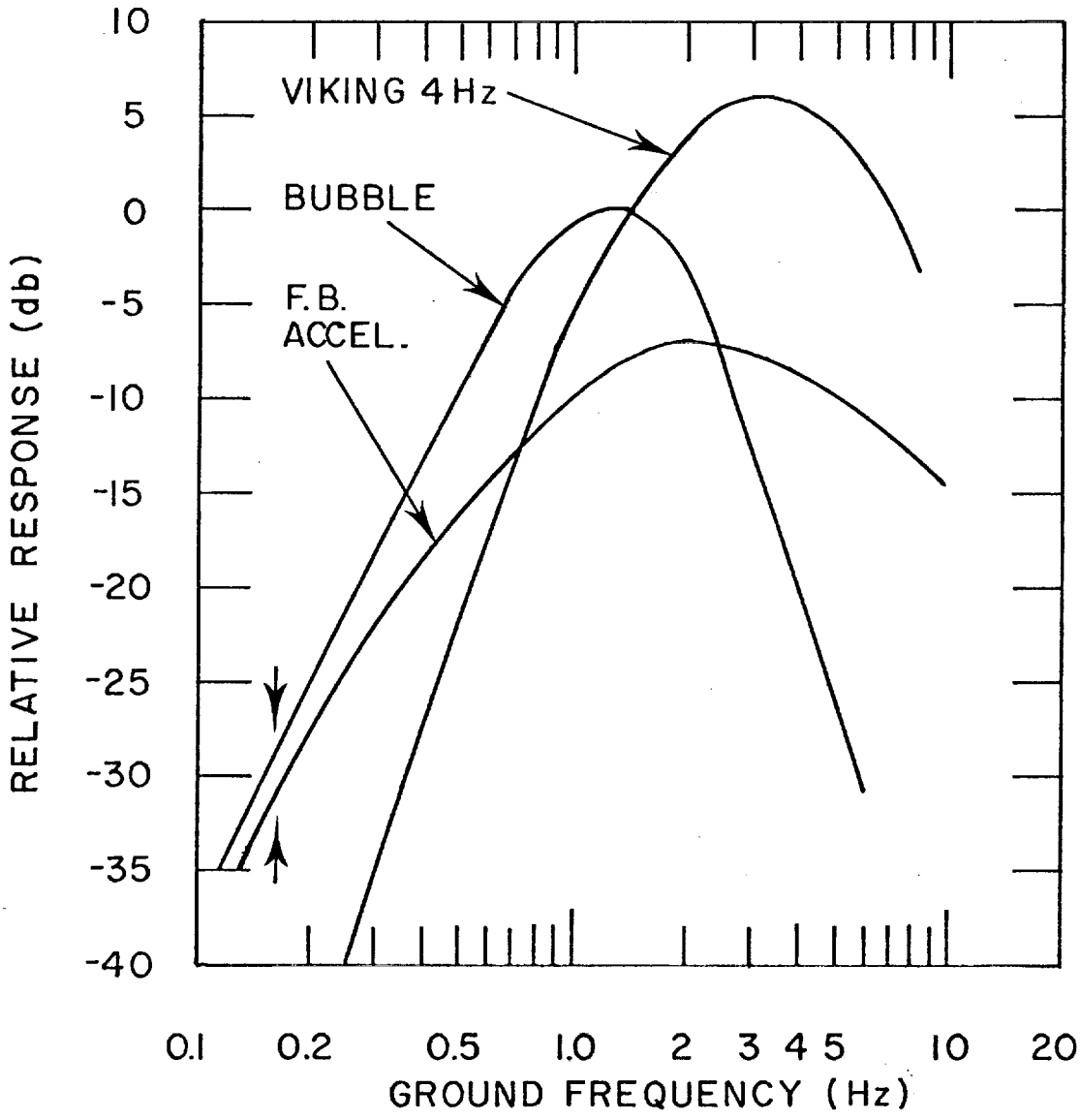

COMPARISON CHARACTERISTICS
AT CIT CAMPUS TEST SITE

FIGURE 11

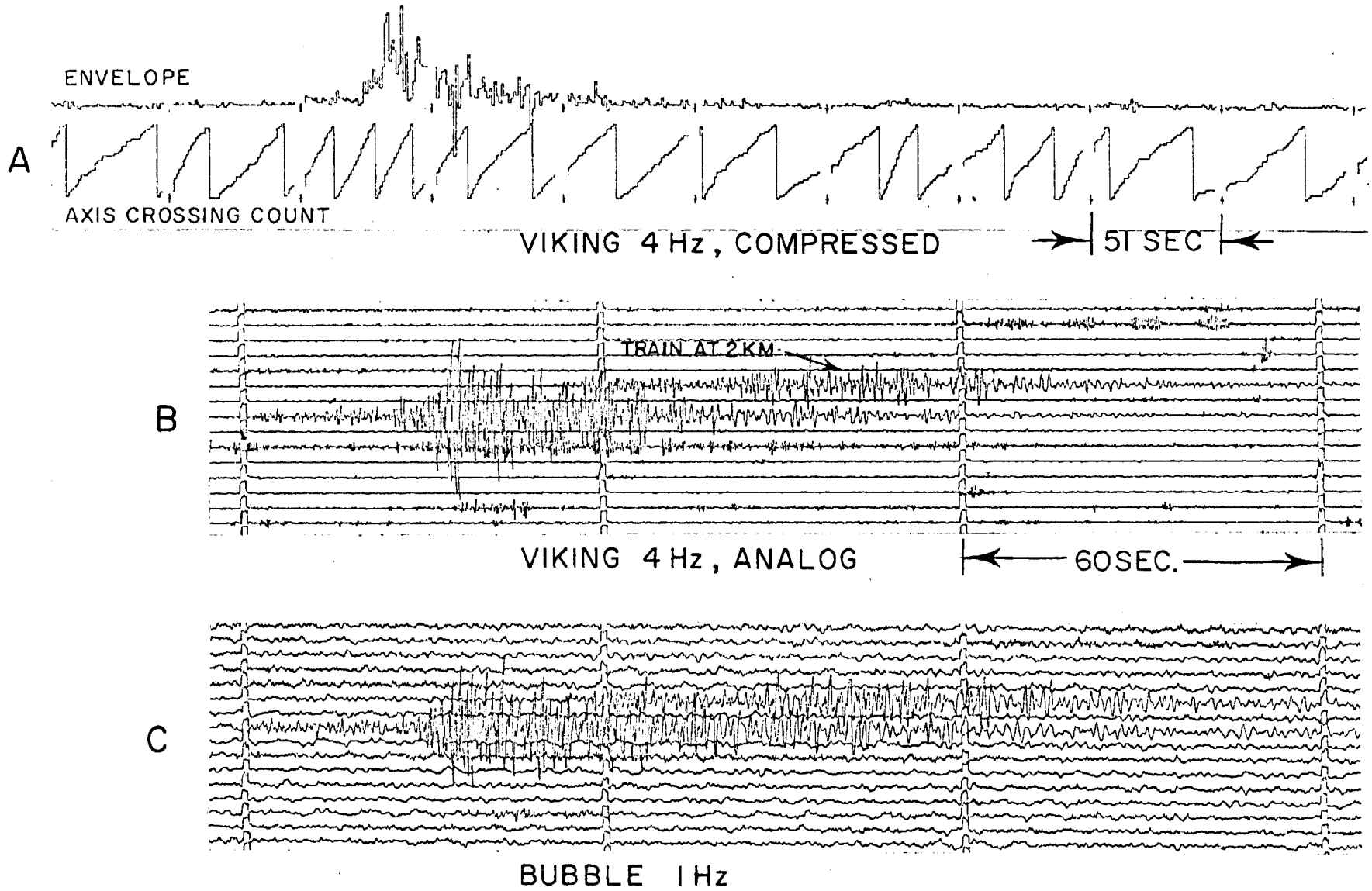

LOCAL EVENT AT 200 KM
RECORD AT CIT CAMPUS TEST SITE

FIGURE 12

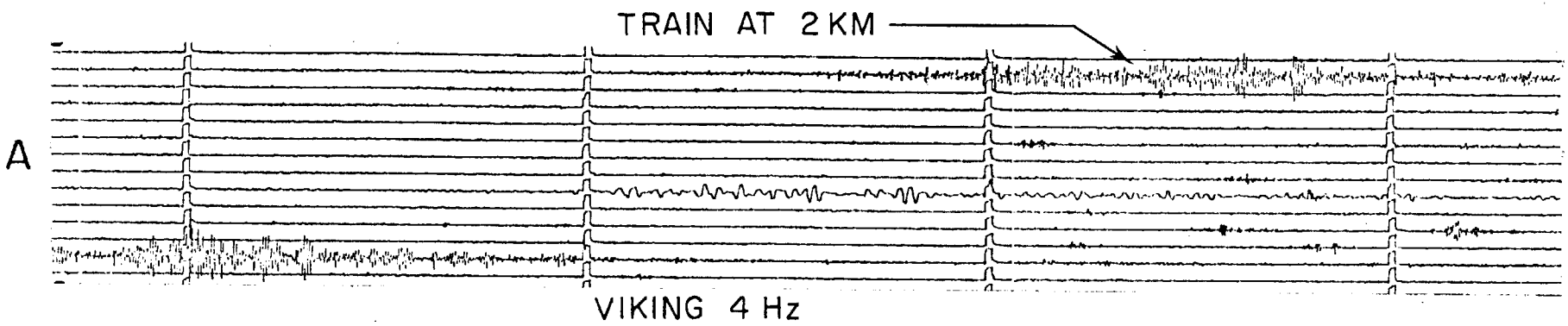

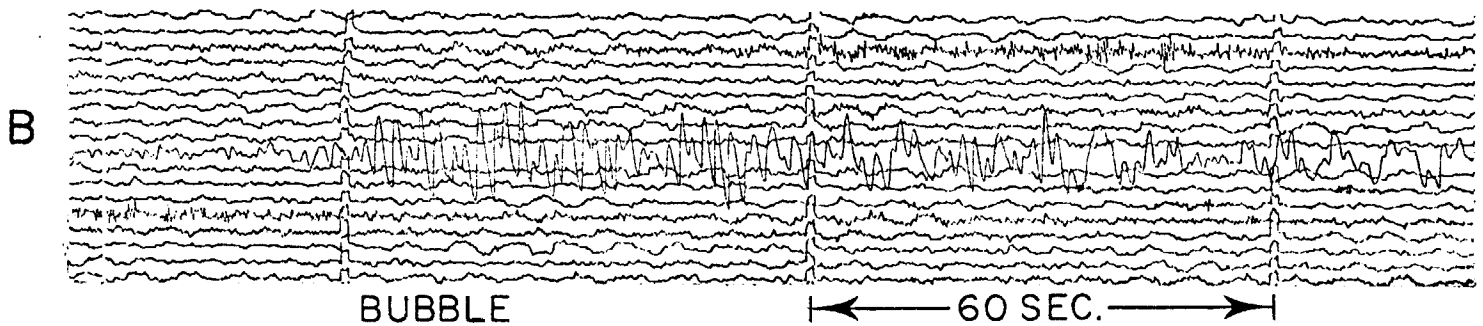

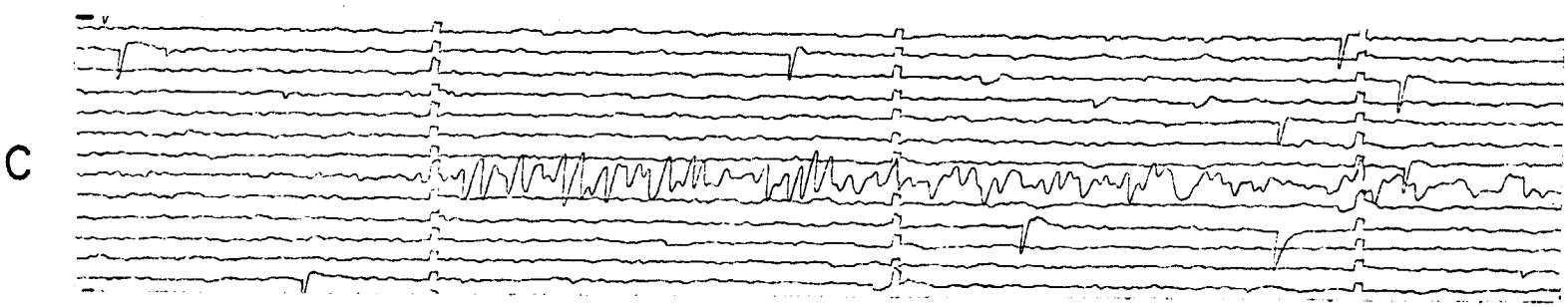

BAJA CALIFORNIA EVENT RECORDED AT CIT CAMPUS TEST SITE

FIGURE 13

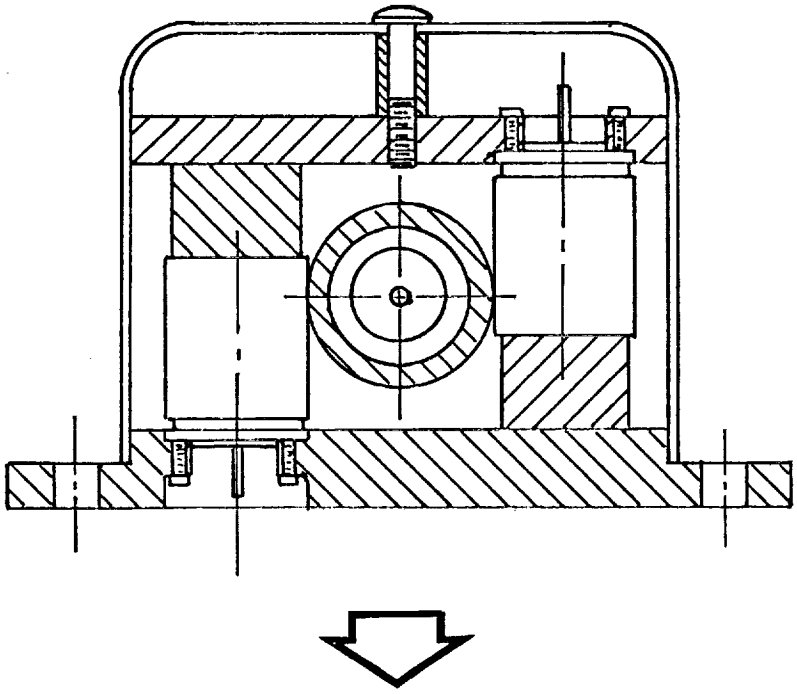

Test jig for shocking stepping motors

FIGURE 14

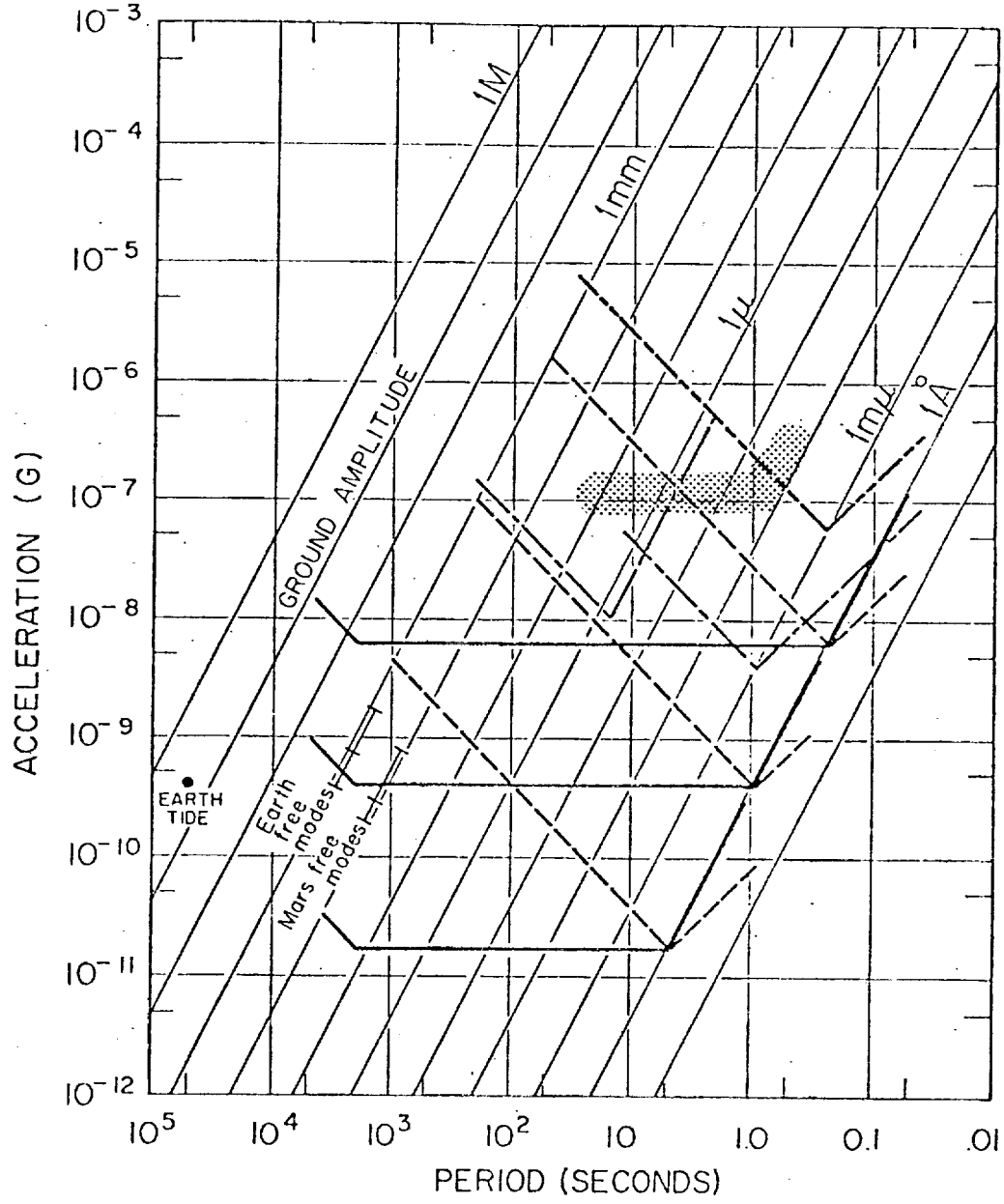

SENSITIVITIES OF SEISMIC SYSTEMS

FIGURE 15